Ballistic Performance of Laminated Functionally Graded Composites of TiB_2-based Ceramic and Ti-6Al-4V Alloy against 14.5 mm heavy machine gun AP of impact velocity 990 $m \cdot s^{-1}$

Jianqiang He and Minquan Wang

Information Management Center, Mechanical Engineering College, Shijiazhuang 050003, China

hejianqiang2016@aliyun.com

Keywords: Laminated composite; continuously-graded microstructure; ballistic performance

Abstract. By inducing thermal explosion in high-gravity field to prepare the laminated composite of TiB_2-based ceramic and Ti-6Al-4V alloy, spatial span-scale continuously-graded microstructure was achieved in interfacial region between the ceramic and Ti alloy, and the formation of the interfacial microstructure resulted from full-liquid ceramic-metal fusion, atomic interdiffusion and subsequent peritectic reaction of TiB_2 primary phases with Ti liquid of graded concentration. By using 14.5 mm AP to conduct DOP test to evaluate ballistic performance of the laminated composite, it was considered that comparing to TiB_2-based ceramic, the presence of spatial span-scale continuously-graded microstructure between the ceramic and Ti alloy brought about the enhanced ballistic performance of the laminated composite by 133.0%.

Introduction

Over the past two decades, a substantial insight has been gained into the dynamic mechanical response of ceramics such as Al_2O_3, SiC, AlN, Si_3N_4 and TiB_2 [1]. The mechanical properties of ceramics have been continuously improved by developing better processing methods and achieving desired microstructures. Hence, one novel armor material of functionally graded armor composites (FGACs) are developing and attract more and more attentions in the field of ordnance material science and engineering. Meanwhile, the fundamental understanding of the mechanisms by which ceramic materials deform during impact loading has been advanced tremendously by development, modification and augmentation of test techniques such as Taylor impact, Kolsky and split-Hopkinson bar, plate impact, explosion cylinder, spherical cavity expansion and so on. However, depth of penetration (DOP) test remains by far the most accepted and predictive method for deriving the ballistic performance of the materials [2]. As a result, DOP tests are often performed to study the characteristics of ballistic penetration in thick ceramic tiles, and small scale and reverse ballistic configurations are also used to conduct such tests[3]. Based on the achievement of laminated functionally graded composite of TiB_2-based ceramic and Ti-6Al-4V alloy by combustion synthesis in high-gravity field, DOP tests are taken to evaluate ballistic performance of the laminated composites, and the mechanisms of the composites defeating the projectile are discussed through comparing to ballistic performance of TiB_2-based ceramic.

Experimental

Raw materials high-purity (>98%) B_4C powder with particle size < 3.0 μm and high-purity (>99%) Ti powder with particle size < 30 μm were used to constitute the primary system as shown in Eq. 1, while Ni and Al powder with purity > 99% and particle size < 30 μm were used to constitute the secondary system as shown in Eq. 2. The mass ratio of Ni-Al secondary system to Ti-B_4C primary system was 1:9.

$$3Ti+B_4C \rightarrow TiC+2TiB_2 \quad (1)$$

$$Ni+Al \rightarrow NiAl \quad (2)$$

The above powders were blended and mechanically activated in ball milling machine for 4h, subsequently, were pressed as the powder compact. After putting the surface-treated discs of Ti-6Al-4V alloy with the diameter 100 mm and the thickness 6 mm at the bottom of the crucibles, the

powder compacts were filling in the crucible. The crucibles were fixed in the rotating arms of the centrifugal machine, then, the centrifugal machine started to make the acceleration at the bottom of crucible be 2000. Followed by that the top of the reaction system was ignited to start thermal explosion reaction in high-gravity field by electrified tungsten wires of diameter of 0.5 mm, the centrifugal machine continued to run for 1 min, then, and it was stoped. As the crucibles were cooled to the ambient temperature, they were removed away from the centrifugal machine, in succession, the samples were taken out of the crucibles. Finally, the hexagonal products of the laminated materials of TiB_2-based ceramic and Ti-6Al-4V alloy were obtained after the samples were worked by electric discharge machining (EDM), as shown in Fig. 1.

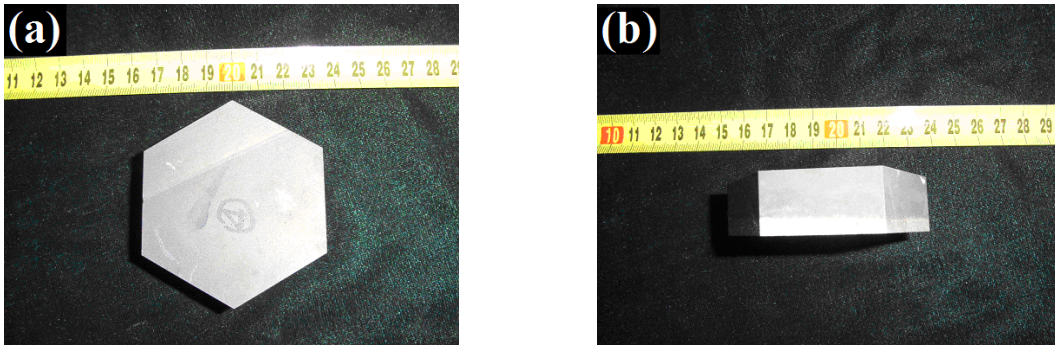

Fig. 1 Hexagonal products of the laminated materials with TiB_2-based ceramic to Ti-6Al-4V alloy (a) front (b) lateral

Fig. 2 The ceramic laterally-confined by steel sleeve

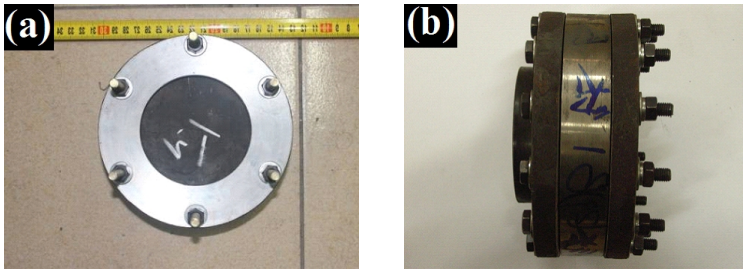

Fig. 3 DOP target of the measure materials (a) front (b) lateral

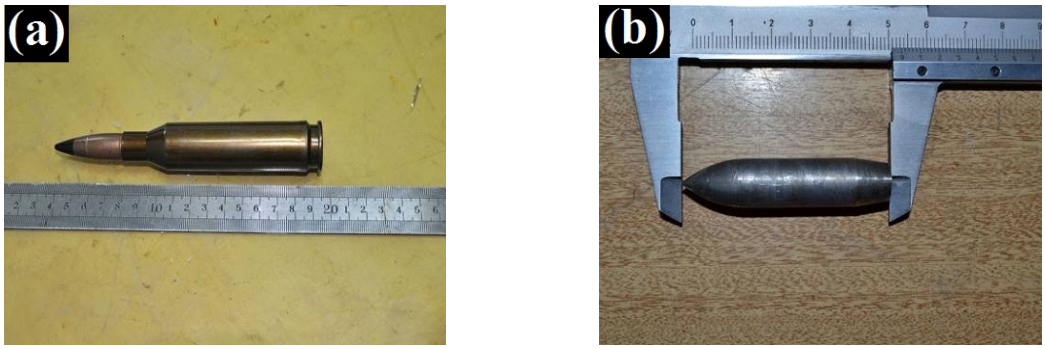

Fig. 4 14.5 mm heavy machine gun armor piercing projectile (a) projectile body (b) quenched steel core of 35CrMoSiA

The discs of TiB_2-based ceramic and the laminated composite were laterally confined by the sleeves of 42CrMo mid-carbon alloy steel, as shown in Fig. 2, respectively, were mechanically covered by thin front plate and thick back plate of quenched 30CrMnSiNi2A high-strength steel to form the target bodies, as shown in Fig. 3. 14.5 mm heavy machine gun armor piercing (AP) projectiles with impact velocity about 1000 $m \cdot s^{-1}$ were used to measure mass effectiveness of the

target materials for evaluating the ballistic performance of the target materials, respective, as shown in Fig. 4, Eq. 3 and Eq. 4.

$$E_m = \frac{[P_s - (P_f + P_b)/m] \cdot r_s}{P_c \cdot r_c} \tag{3}$$

$$m = P_0 / P_s \tag{4}$$

in which P_0 was the depth of penetration of armor steel against 14.5 mm armor piercing projectile of impact velocity (V) 990 m·s^{-1} (about 42 mm), P_f was the thickness of the front plate, P_b was residual penetration depth in back plate; m was the conversion coefficient of thickness of front plate and back plate material relative to the armor steel (about 0.74), ρ_s was the density of armor steel (as 7850 kg·m^{-3}), P_c was the penetration depth in the measured material, ρ_c was the density of the measure material.

Results and Discussion

Phase constitution and microstructure at interface. Low-magnification FESEM images showed that there was not sharp interface but gradual microstructure evolution from the ceramic to Ti-6Al-4V substrate, as shown in Fig. 5. By cutting the sample into the several pieces at interval 0.5 mm from the ceramic to Ti-6Al-4V substrate, XRD and FESEM results showed that TiB_2 platelets rapidly decreased until they disappeared completely in interfacial region, while TiB platelets arose around the ceramic matrix and increased in interfacial region, however, TiB platelets decreased gradually instead as the interfacial region was close to Ti-6Al-4V substrate, as shown in Fig. 6 and Fig. 7.

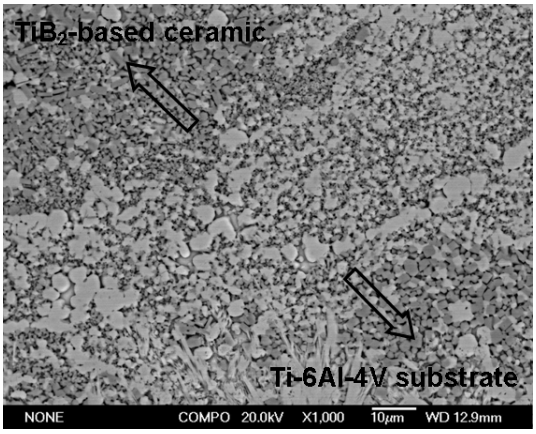

Fig. 5 Low-magnification FESEM image of interfacial region from the ceramic to Ti-6Al-4V substrate

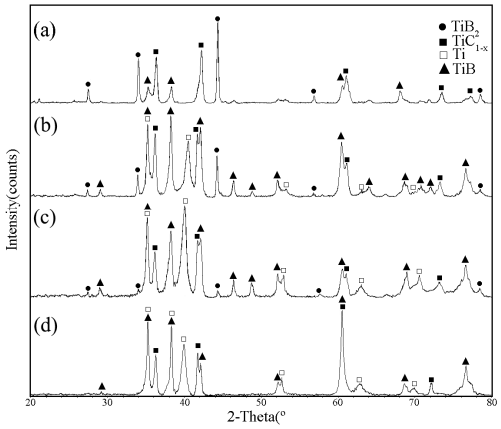

Fig. 6 XRD patterns of interfacial region from the ceramic to Ti-6Al-4V substrate (a) ceramic matrix (b) the area of 0.5 mm away from the ceramic (c) the area of 1.0 mm away from the ceramic Ti alloy (d) the area of 1.5 mm away from the ceramic

According to the literatures [4], high-gravity field accelerates liquid products to deposit toward the unreacted powder compact, and promotes liquid products to infiltrate into the cavities in the powder compact, thereby enhancing the inter-diffusion of reactive components in reaction system. As a result, high heat accumulation yields high energy concentration during reaction process so that thermal explosion mode arises in high-gravity field. The presence of thermal explosion not only makes high-temperature full-liquid products achieved, but also causes Ti-6Al-4V substrate to be partially molten, subsequently, so intensive atomic interdiffusion takes place among the liquid products (such as TiB_2 and TiC) and the molten Ti-6Al-4V alloy, and the respective concentration gradients of the elements (such as Ti, B, C and so on) develop among the liquid products and Ti-6Al-4V substrate. Subsequently, at final stage of interfacial solidification TiB_2 primary phases more and more participate in peritectic reaction in the presence of Ti concentration gradient until TiB_2 primary

phases entirely transform a number of fine TiB solids in interfacial region, so spatial span-scale continuously-graded microstructure develops in interfacial region between solidified Ti-based ceramic and Ti-6Al-4V substrate, as shown in Fig. 6 and Fig. 7.

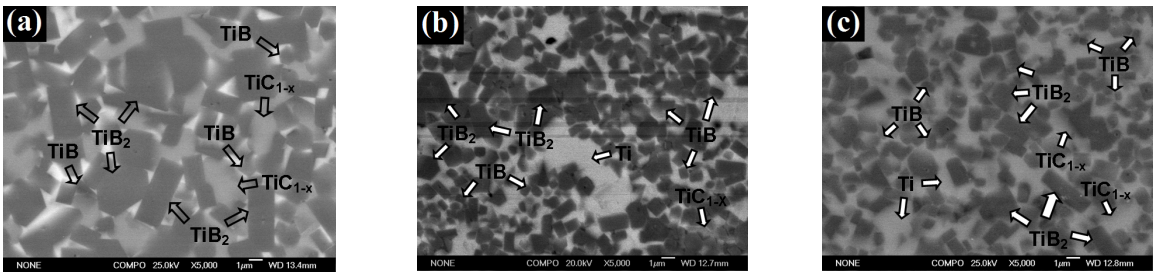

Fig. 7 High-magnification FESEM images of the interfacial region from the ceramic to Ti-6Al-4V substrate (a) the ceramic matrix (b) the area of 0.5 mm away from the ceramic (c) the area of 1.0 mm away from the ceramic

Ballistic performance of the laminated composite. The ballistic performance of the laminated composite of TiB_2-based ceramic and Ti-6Al-4V alloy were evaluated by DOP test, and mass effectiveness of the composite comparing to TiB_2-based ceramic against 14.5 mm armor piercing (AP) projectiles were calculated by using the Eq. 3 and Eq. 4, as shown in Table 1. As could be seen, mass effectiveness of TiB_2-based ceramic obtained in current experiment somewhat exceeded one of hot-press sintering TiB_2 monolithic ceramic against 14.5 mm heavy gun machine AP [1], in contrast, comparing to TiB_2-based ceramic, the laminated composite of TiB_2-based ceramic and Ti-6Al-4V alloy was enhanced in mass effectiveness by 133.0%, so it was promised the laminated composite could present the inherent high ballistic performance.

Table 1 DOP ballistic performance of the laminated composite compared by TiB_2-based ceramic

materials	ρ_c [10^3×kg·m^{-3}]	V [m·s^{-1}]	P_f [mm]	P_b [mm]	P_c [mm]	m	E_m
TiB_2-based ceramic	4.40	989	2	1.4	19	0.74	3.39
Laminated composite	4.45	990	2	—	8.5	0.74	7.90

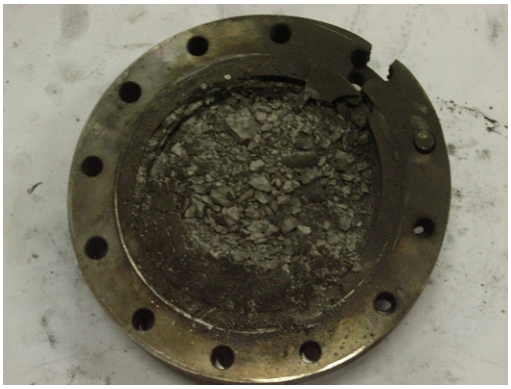

Fig. 8 Damage image of the target composed of TiB_2-based ceramic

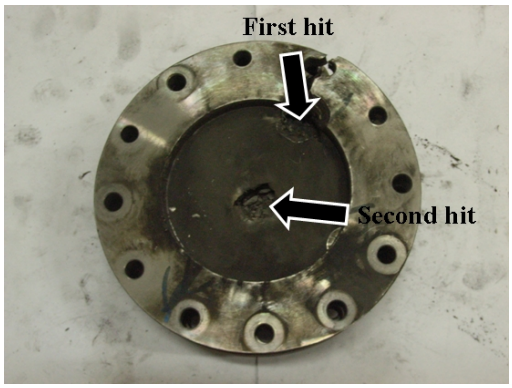

Fig. 9 Damage image of back plate of high-strength steel

The damage image of the target composed of TiB_2-based ceramic was showed in Fig. 8, the target was perforated in the presence of twice impact, and the crater of the depth 1.4 mm remained in the back plate of quenched 30CrMnSiNi2A high-strength steel, as shown in Fig. 9. In contrast, for the target comprised of the laminated composite, after it was impacted by the common projectile at near-same impact velocity, the target had not yet been perforated, and the crater of the depth 8.5

remained in the ceramic part of the laminated composite, as shown in Fig. 10, reversely, the projectile damaged severely, i.e. the top of the projectile was blunted seriously while the projectile body was broken down, as shown in Fig. 11.

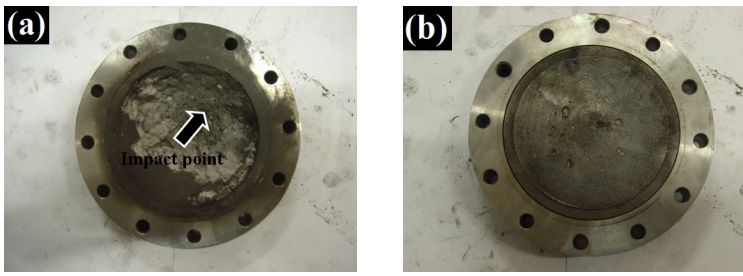

Fig. 10 Damage image of the target comprised of laminated composite (a) front (b) back

Fig. 11 Damage image of the projectile after DOP

According to the current achievement in dynamic fracture of ceramics [5], it is well known that because of the formation and development of the reflected tensile stress wave from the back plate, failure initiated from the back side of the ceramic tile for a typical thin-layered system consisting of a ceramic plate and a metal or textile backing plate bound together with a thin adhesive layer. Wilkins et al .[6] observed that initial cracks in ceramic tiles do not significantly affect the penetration resistance of the target as long as the projectile does not impact on or very close to the cracks, and it takes time for the cracked or damaged zone to develop from the back surface to the impact surface. However, when the damaged zone reaches the projectile and the damaged area is comparable to the projectile cross section, the ceramic tile fails. Before the damaged zone reaches the projectile, the projectile is unable to penetrate. This time of non-penetration is known as dwell. If the projectile is short, this damage development time may be sufficiently long, such that the projectile has completely deformed plastically or shattered before the damaged zone reaches the impact surface. In this case, no penetration occurs, which is called interface defeat.

Meanwhile, by presented an exact solution for the transmission of spherical waves across planar surfaces, Furlong et al [7] considered the coefficient of reflection and refraction depended not only on the acoustic impedances of the media, but also on the boundary conditions at the interface, the wave face curvature and the source frequency. As a result, three types of boundaries can exist: the first one is free, as with a free standing ceramic plate; the second one is no shear-coupling, as with two unbonded or lightly bonded plates; the third one is shear-coupling, where good adhesion or coupling exists, allowing the transmission of transverse motion and stress. The latter shear-coupled or no slip condition provides the best interface for a ceramic-metal design, and Leighton et al [8] considered the enhanced ballistic performance of laminated ceramic-titanium composites resulted from increased interlayer bond strength (strong, shear-coupled metallurgical bonds).

Hence, it is just the presence of spatial span-scale continuously-graded microstructure from the ceramic to Ti-6Al-4V substrate that high interfacial bond strength (i.e. 235 ± 25 MPa) is presented between TiB_2-based ceramic and Ti-6Al-4V substrate. As a result, the compressive load transfer is enhanced from the ceramic to Ti-6Al-4V substrate, whereas the intensity of reflected tensile stress wave is reduced and the damage inside the ceramic is mitigated during DOP test. More importantly, the transmission of transverse motion and stress at the interface is also restrained through yielding shear-coupling effect, not only bringing about the increased dwell of the projectile inside the ceramic, but more importantly cause the failure of the ceramic matrix to be retarded. Finally, enhanced ballistic performance of the laminated composite is presented.

Summary

By inducing thermal explosion of combustion synthesis in high-gravity field to prepare the laminated composite of TiB_2-based ceramic and Ti-6Al-4V substrate, spatial span-scale continuously-graded microstructure was observed clearly from the ceramic to Ti-6Al-4V alloy, and the interfacial microstructure evolution resulted from ceramic-metal fusion, atomic interdiffusion and subsequent

peritectic reaction of TiB_2 primary phases with Ti liquid. By preparing two kinds of confined targets composed of TiB_2-based ceramic and the laminated composite respectively, DOP test was taken to evaluate ballistic performance of measured materials. It is considered that the presence of spatial span-scale continuously-graded microstructure in the interfacial region between the ceramic and Ti-6Al-4V alloy, not only enhances compressive load transfer from the ceramic to Ti alloy, reduces the intensity of the reflected tensile stress wave to mitigate the damage inside the ceramic, but also more importantly restrains the transmission of transverse motion and stress at the interface through yielding shear-coupling effect, thereby presenting the increased dwell of the projectile inside the ceramic, finally, the failure of the ceramic in the laminated composite is retarded. As a result, comparing to TiB_2-based ceramic (mass effectiveness 3.39 against 14.5 mm heavy machine gun AP projectile), the ballistic performance of the laminated composite is enhanced by 133.0%.

References

[1] B. James, Practical issue in ceramic armor design, Ceramic Armor Materials by Design 134 (2002) 23-31.

[2] D. M. Stepp, Damage mitigation in ceramics: historical developments and future directions in army research, Ceramic Armor Materials by Design 134 (2002) 421-428.

[3] D. L. Orphal, R. R. Franzen, A. C. Charters, T. L. Menna and A. J. Piekutowski, Penetration of confined boron carbide targets by tungsten long rods at impact velocities from 1.5 to 5.0 km/s, Int. J. Impact. Eng. 9 (1997) 15-29.

[4] V. I. Yukhvid, Effect of convective motion on the flame structure in combustion waves propagating in heterogeneous systems under natural and artificial Gravity Conditions, Com bustion, Explosion and Shock Waves 45 (2009) 421-427.

[5] W. W. Chen, A. M. Rajendran, B. Song and X. Nie, Dynamic fracture of ceramics in armor applications, J. Am. Ceram. Soc., 90 (2007) 1005-1018.

[6] T. J. Holmquist, G. R. Johnson, Modeling prestressed ceramic and its effect on ballistic performance, Inter. J. Impact. Eng. 31 (2005) 113-127.

[7] J. Furlong, C. Westbury and E. Phillips, A method for predicting the reflection and refraction of spherical wave across planar interfaces, J. Applied. Physics. 76 (1994) 128-136.

[8] W. A. Gooch, An overview of ceramic armor application, Ceramic Armor Materials by Design 134 (2002) 3-21.